The N-Terminal Repeat Domain of α-Synuclein Inhibits β-Sheet and Amyloid Fibril Formation†

Jeffrey C. Kessler, Jean-Christophe Rochet, and Peter T. Lansbury, Jr.*

Center for Neurologic Diseases, Brigham and Women's Hospital, and Department of Neurology, Harvard Medical School, 65 Landsdowne Street, Cambridge, Massachusetts 02139

Received June 24, 2002

ABSTRACT: The conversion of α-synuclein into amyloid fibrils in the *substantia nigra* is linked to Parkinson's disease. α-Synuclein is natively unfolded in solution, but can be induced to form either α-helical or β-sheet structure depending on its concentration and the solution conditions. The N-terminus of α-synuclein comprises seven 11-amino acid repeats (XKTKEGVXXXX) which can form an amphipathic α-helix. Why seven repeats, rather than six or eight, survived the evolutionary process is not clear. To probe this question, two sequence variants of α-synuclein, one with two fewer (del2) and one with two additional (plus2) repeats, were studied. As compared to wild-type α-synuclein, the plus2 variant disfavors the formation of β-sheet-rich oligomers, including amyloid fibrils. In contrast, the truncated variant, del2, favors β-sheet and fibril formation. We propose that the repeat number in WT α-synuclein represents an evolutionary balance between the functional conformer of α-synuclein (α-helix and/or random coil) and its pathogenic β-sheet conformation. N-Terminal truncation of α-synuclein may promote pathogenesis.

Symptoms of Parkinson's disease (PD)[1] include difficulty in initiating movement, rigidity, and resting tremor (*1*, *2*). Post-mortem PD brains are characterized by intraneuronal cytoplasmic inclusions known as Lewy bodies (LB) in the *substantia nigra*, the area of most severe neuronal loss. The fibrillar structures that comprise the inclusions consist predominantly of α-synuclein (*3*−*6*), a presynaptic protein of unknown function that is highly expressed throughout the brain (*7*−*11*). The involvement of α-synuclein in PD pathogenesis was first suggested by studies of families with autosomal dominant early-onset PD (FPD) in which two separate mutations in the α-synuclein gene, A53T and A30P, were linked to disease (*12*, *13*). This linkage suggests that α-synuclein might also be involved in idiopathic PD, from which cases of FPD are nearly indistinguishable, with the exception of the age of disease onset (*14*−*16*).

Both FPD mutations alter the rate of α-synuclein aggregation in vitro (*17*), but only the A53T mutation accelerates fibril formation as compared to WT (*18*−*22*). Both mutations accelerate the appearance of protofibrils, suggesting a link between protofibrils and disease. Transgenic mice overexpressing human α-synuclein show changes similar to those seen with PD, including the age-dependent appearance of neuronal inclusions and motor deficits (*23*, *24*). Inclusions in these mice are not fibrillar, again suggesting that fibrils may not be pathogenic. Recently, the brains of α-synuclein transgenic mice were demonstrated to contain insoluble, truncated forms of α-synuclein only in regions where neurodegeneration was observed (*25*). The significance of this truncation to PD has not been established.

Little is known about the normal function of α-synuclein. It is highly expressed in the brain, but mice lacking α-synuclein are qualitatively normal, showing only small increases in the rate of dopamine release during paired stimuli (*26*). In vitro studies have shown that the protein is natively unfolded in solution and remains soluble when boiled (*27*). Whether its conformational flexibility is important for its function is not understood.

The N-terminal domain of α-synuclein contains seven positively charged 11-mer repeats (XKTKEGVXXXX consensus motif) (Figure 1A). When mixed with lipid vesicles comprising negatively charged phospholipids, HFIP, or SDS, α-synuclein assumes an α-helical conformation (*27*, *28*). The repeats are required for both helical induction and lipid vesicle binding (*29*, *30*).

Sequence repeats are a feature of several proteins associated with neurodegenerative diseases that are characterized by protein aggregation. Huntingtin, the protein that, in expanded form, is linked to Huntington's disease, normally contains a polyglutamine repeat. There is a strong correlation between the length of the expanded polyglutamine tract, the age of disease onset, and the rate of in vitro fibril formation by polyglutamine-containing model peptides (*31*, *32*). Tau, a protein associated with frontotemporal dementia and Alzheimer's disease, contains repeats that affect its polymerization rate (*33*, *34*). One form of genetic prion disease is caused by the insertion of additional copies of an octapeptide

† This work was supported by a Morris K. Udall Parkinson's Disease Research Center of Excellence Grant from the National Institutes of Health (NS 38375).

* To whom correspondence should be addressed. Telephone: (617) 768-8610. Fax: (617) 768-8606. E-mail: plansbury@rics.bwh.harvard.edu.

[1] Abbreviations: A30P, human A30P α-synuclein; A53T, human A53T α-synuclein; CD, circular dichroism; DTT, dithiothreitol; EM, electron microscopy; FPD, familial Parkinson's disease; HFIP, 1,1,1,3,3,3-hexafluoro-2-propanol; NAC, nonamyloid component of Aβ; PBS, phosphate-buffered saline; PD, Parkinson's disease; PMSF, phenylmethanesulfonyl fluoride; PrP, prion protein; TBS, Tris-buffered saline; TMAO, trimethylamine *N*-oxide; WT, human wild-type α-synuclein.

10.1021/bi020429y CCC: $25.00
Published on Web 12/28/2002

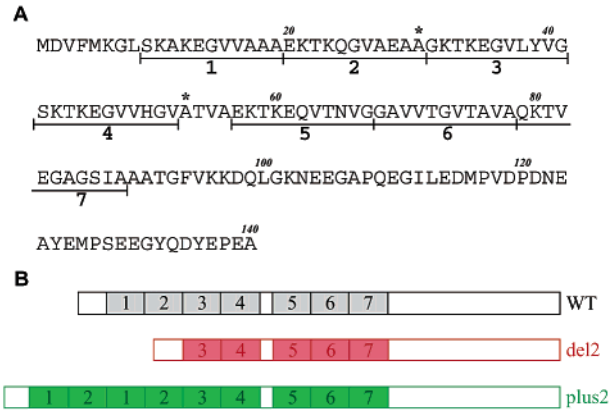

FIGURE 1: Amino acid sequence of α-synuclein and schematic representation of the variants. (A) The underlined regions mark the 11-mer repeats. Asterisks mark the residues (A30P and A53T) mutated in FPD. (B) Representation of WT (black) and the two variants, del2 (red) and plus2 (green). The shaded regions represent the 11-mer repeats; the numerical labels indicate the order of the repeats in WT. Del2 lacks the first two repeats found in WT (residues 9−30); plus2 has two copies of the first two repeats (residues 9−30 are repeated in tandem).

repeat near the prion protein (PrP) N-terminus (*35*−*37*). The biological functions of the normal, repeat sequences are not known, but we expect that they exist, since it is otherwise difficult to imagine why they are conserved.

To investigate the role of the repeats in the conformational properties of α-synuclein, two variants with an altered number of repeats were created, one with two additional 11-mer repeats (plus2) and one with two fewer repeats (del2) (Figure 1B). Del2 may be related to as-yet-unidentified truncated forms of α-synuclein found in PD mouse models (*25*). Various biochemical and biophysical techniques were used to evaluate conformational differences between these variants and wild-type α-synuclein (WT). This comparison suggests that the repeats decrease the tendency of the protein to form *β*-sheet structures, including protofibrils and fibrils.

EXPERIMENTAL PROCEDURES

Cloning. The two α-synuclein variants del2 and plus2 (Figure 1) were generated from the human α-synuclein cDNA and were cloned into the pT7-7 *Escherichia coli* expression vector (provided by S. Tabor, Harvard Medical School). Del2 α-synuclein, which was generated using PCR, lacks bases 25−90 encoding the first two 11-mer repeats (residues 9−30). The gene encoding the plus2 variant has a second copy of residues 25−90 inserted in tandem with the existing one. These repeats were inserted by generating a silent mutation (T54A) using site-directed mutagenesis (Quikchange mutagenesis kit, Stratagene) creating a *Pst*I site in the α-synuclein cDNA. Two complementary single-stranded oligonucleotides, containing the sequence of the first two repeats with PstI ends, were annealed together and ligated into the *Pst*I site.

Expression and Purification. Cells of *E. coli* strain BL-21 DE-3 were transformed with the expression vectors for each construct, and expression was induced by the addition of isopropyl D-thiogalactopyranoside. The purification procedure that was used was a modified version of published protocols (*18*, *27*). Cells were harvested, resuspended in 10 mM Tris (pH 7.5), 1 mM EDTA, 1 mM PMSF, and 1 mM DTT ($^1/_{10}$ culture volume), and lysed by freezing in liquid nitrogen followed by thawing and either probe sonication or passage through a French cell press (twice). After the lysate had been treated with streptomycin sulfate and ammonium sulfate, the protein was then resuspended in a minimal volume of 10 mM Tris (pH 7.5) and 0.5 M NaCl and boiled for 20 min. The supernatant was saved, concentrated, and exchanged into 10 mM Tris (pH 7.5). The protein was loaded onto a Sephacryl S-300 size-exclusion column (Pharmacia) and eluted in 100 mM NH_4HCO_3. α-Synuclein-containing fractions, identified by Coomassie-stained SDS−PAGE, were combined and lyophilized.

Circular Dichroism Spectroscopy. Far-UV CD spectra of α-synuclein were collected at 22 °C using an Aviv 62A DS spectropolarimeter and a 0.1 or 0.02 cm cuvette. The data were acquired at 1 nm intervals, with a response time of 10 s per measurement. The final spectra were obtained by calculating the mean of three individual scans and subtracting the background.

Titration curves were generated by taking measurements at a single wavelength (222 nm for α-helix and 218 nm for *β*-sheet) every second for 120 s, using a response time of 1 s per measurement. Each point on a titration curve was the mean of the 120 sample points.

Deconvolution of CD Spectra. The software program CDFit (B. Rupp, Lawrence Livermore National Laboratory, Livermore, CA) was used to estimate the amount of α-helix, *β*-sheet, and random coil from far-UV CD spectra. This program uses least-squares minimization to fit CD spectra to a linear combination of standard polylysine curves for α-helix, *β*-sheet, and random coil (*38*).

Trimethylamine N-Oxide Titration. A 6 M stock of TMAO was prepared in PBS or TBS [10 mM Tris and 150 mM NaCl (pH 7.5)] and mixed with 60 *μ*M protein in a 2:1 ratio (v/v) to generate a solution containing 20 *μ*M protein in 4 M TMAO. This was mixed at various ratios with 20 *μ*M protein in PBS or TBS to generate a 20 *μ*M protein solution in TMAO concentrations ranging from 0 to 4 M. These solutions were incubated at room temperature for 24 h and then analyzed by far-UV CD spectroscopy.

1,1,1,3,3,3-Hexafluoro-2-propanol Titration. HFIP was added to a 60 *μ*M solution of protein in TBS at concentrations ranging from 0 to 8% HFIP and diluted in TBS to a final concentration of 50 *μ*M protein. These samples were then analyzed by far-UV CD spectroscopy after incubation at room temperature for 24 h.

Preparation of α-Synuclein Incubations for Fibrillization Studies. Samples were dissolved in TBS with 0.02% sodium azide and filtered through a 0.22 *μ*m filter followed by a Microcon 100K molecular weight cutoff filter (Millipore). Protein concentrations in the filtrate and incubation were determined by UV absorbance and quantitative amino acid analysis (*17*). Samples were incubated at 37 °C on a roller drum, rotating at 60 rpm. Due to the variability between experiments in the lag time of aggregation, typical results are shown.

Thioflavin T Fluorescence Assay for Fibril Formation. Aliquots of the α-synuclein incubations were assayed by thioflavin T (thio T) fluorescence as described previously (*18*).

Electron Microscopy. The EM samples were prepared by placing 10 *μ*L of the α-synuclein solution on a carbon-coated grid and allowing the solution to stand for 1 min before

removing the excess solution. The grid was then washed once with distilled water and once with 1% uranyl acetate before the sample was stained with fresh 1% uranyl acetate for an additional 2 min. The samples were then studied in a Joel-1200EX electron microscope. The grids were thoroughly examined to obtain an overall statistical evaluation of the structures present in the sample. All electron micrographs were taken at 80 kV.

Gel Filtration and UV Absorbance Measurements. To measure the amount of monomer in each fibrillization reaction mixture, 20 μL aliquots were periodically removed, centrifuged at 16000*g* for 5 min to remove insoluble material, and injected onto a Shodex KW-G column (Showa Denko, Japan) to isolate the monomeric protein. Elution was monitored by UV absorbance at 220 nm, and peak areas were calculated to determine the amount of monomer in each sample. To correct for small ($<5\%$) differences in the extinction coefficients, ratios between extinction coefficients at 220 and 280 nm were measured for each variant, and the peak areas were correspondingly adjusted, as extinction coefficients are theoretically the same for all three proteins at 280 nm (*39*), which was confirmed by amino acid analysis. All other gel filtration chromatography was performed on a Superdex 200 column (Amersham).

RESULTS

Cloning, Expression, and Purification of α*-Synuclein Variants: WT, Plus2, and Del2.* PCR was used to delete the portion of the α-synuclein cDNA encoding the first two N-terminal repeats, generating the del2 variant (Figure 1B). PCR could not be used to generate the plus2 variant since proper hybridization of primers containing a repeated sequence would not be assured. Instead, a silent mutation (T54A) was created in the α-synuclein cDNA to generate a restriction site (*Pst*I), and a small oligonucleotide containing the repeat sequence was ligated into this site. Correct sequences were confirmed; they were then expressed in *E. coli* and purified by a protocol identical to that used for WT. Purified WT can be prepared by boiling the *E. coli* lysate (*27*); the same result was observed for plus2 and del2 (not shown). After purification, the lyophilized proteins were assayed by SDS−PAGE and amino acid analysis. Both procedures demonstrated high purity ($\geq 95\%$) of the proteins. Plus2 and del2 were reactive with the α-synuclein antibodies 7071, syn-1, and LB-509 by Western blot analysis (Supporting Information).

All Three α*-Synuclein Variants Are Natively Unfolded.* Like WT, when plus2 and del2 were eluted from a gel filtration column, most of the protein was monomeric, with a small amount of protofibrillar material in the void volume (Supporting Information). As previously observed, the retention time of monomeric WT, a 14 kDa protein, was consistent with that of a ca. 60 kDa globular protein (*27*). Plus2 and del2 eluted with similar mobilities, del2 slightly later (34 min) than WT (33 min) and plus2 slightly earlier (32 min). Monomeric proteins were isolated by gel filtration and analyzed by CD spectroscopy (Supporting Information). The resulting spectra were very similar, all characteristic of a random coil structure with a minimum at 198 nm. Both variants remained soluble when boiled and displayed the same CD spectra before and after boiling (data not shown), also consistent with a natively unfolded protein (*27*).

N-Terminal Repeats Inhibit β*-Sheet Formation.* To investigate differences in secondary structure potential among the variants, structure induction by TMAO and HFIP was studied. TMAO is an osmolyte that typically causes unfolded or denatured globular proteins to fold into their native globular structures (*40*, *41*). Far-UV CD spectra of the three proteins were recorded in 2 and 4 M TMAO. At 2 M TMAO (Figure 2A), all three proteins were partially folded and contained different amounts of α-helix (35% in WT, 14% in del2, and 49% in plus2) and β-sheet (24% in WT, 42% in del2, and 1% in plus2). When the TMAO concentration was increased to 4 M (Supporting Information), the amount of β-sheet structure in all three variants was significantly increased (56% in WT, 73% in del2, and 49% in plus2).

The transition from random coil to a β-sheet-rich structure by each variant was compared by measuring the ellipticity at 218 nm over a range of TMAO concentrations (Figure 2B, ellipticity values normalized to the maximum value observed for each protein). In each case, the transition was highly cooperative, consistent with a two-state transition. The del2 variant converted to the β-sheet species more easily (at a lower TMAO concentration) than WT or plus2.

N-Terminal Repeats Are Important for Helix Formation. HFIP was used to induce the conversion of each variant to an α-helical structure. Like WT, both variants assumed spectra characteristic of fully α-helical proteins at 8% HFIP (Supporting Information), with minima at 208 and 222 nm. However, at 4% HFIP (Figure 2C), only WT and plus2 were predominantly α-helical (75% in WT, 0% in del2, and 95% in plus2), whereas del2 contained substantial β-sheet structure (10% in WT, 61% in del2, and 0% in plus2). Furthermore, at 3% HFIP (Supporting Information), WT and del2 contained substantial β-sheet structure (58% in WT and 49% in del2), whereas plus2 was mostly α-helix (29%) and random coil (60%), with only a small amount (11%) of β-sheet.

These data suggested that del2 was significantly more reluctant to form α-helical structure than the other two variants, a conclusion that was supported by an HFIP titration (ellipticity at 222 nm was measured, Figure 2D). The curves were normalized for maximum structural induction, as for the TMAO titration. The plus2 variant underwent a cooperative transition from random coil to α-helix. In contrast, WT and del2 both seemed to populate an intermediate state between random coil and fully α-helical. This state is more pronounced for del2, consistent with the emerging theme that truncation of repeats stabilizes β-sheet structure.

N-Terminal Repeats Inhibit Amyloid Fibril Formation. Solutions of plus2, del2, and WT were filtered to remove oligomeric seeds, and incubated on a rotating drum at 37 °C. Aliquots were removed from each solution periodically and assayed by (1) thio T fluorescence, to detect amyloid fibrillar material, (2) UV absorbance measurements (after centrifugation and gel filtration), to detect monomeric protein, (3) CD spectroscopy, to monitor changes in secondary structure, and (4) electron microscopy (EM), to determine oligomer morphology. In each case, amyloid fibril formation (Figure 3A and Supporting Information) paralleled the loss of monomer from solution (Figure 3B). Consistent with its greater propensity to form β-sheet structure, the del2 variant fibrillized more rapidly than either plus2 or WT. Although lag times for fibrillization are difficult to control and vary from experiment to experiment, four separate del2 incuba-

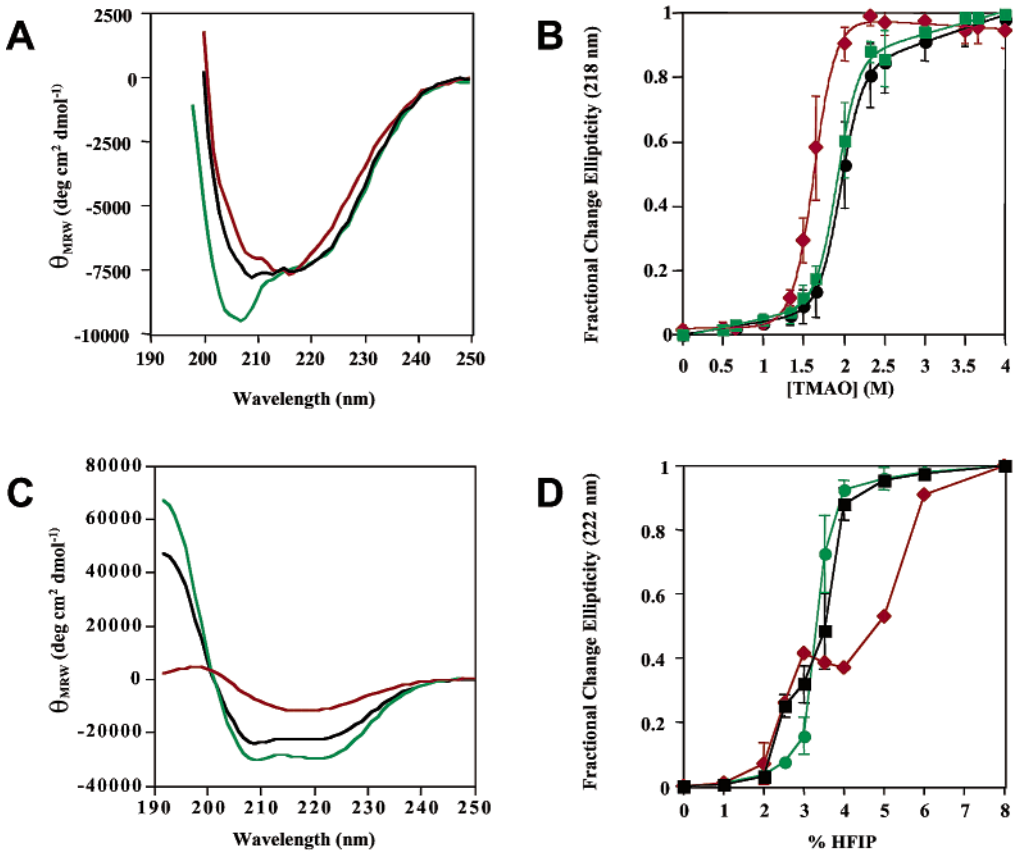

FIGURE 2: Far-UV CD spectra and titrations of WT and the variants under various solvent conditions. (A) α-Synuclein and variants (20 μM) in 10 mM Tris (pH 7.5), 150 mM NaCl, and 2 M TMAO: WT (black), del2 (red), and plus2 (green). (B) Incubations over a range of TMAO concentrations. Ellipticity was measured at 218 nm. Each curve was normalized so that the value at zero was set to the ellipticity at 218 nm with 0 M TMAO and the value at 1 is set to the (absolute) maximal value of ellipticity measured at any concentration for each variant. Del2 forms β-sheet at lower TMAO concentrations than either WT or plus2. (C) Protein (50 μM) in 4% HFIP. (D) Incubations over a range of HFIP concentrations at 222 nm. Stabilization of β-sheet at 3−4% HFIP is strongest in del2, weaker in WT, and absent in plus2. Curves were normalized as described for the TMAO titration.

tions first showed a positive thio T signal at 11−21 h, while WT incubations did not show a significant thio T signal until 30−45 h (Figure 3A and Supporting Information). Plus2 incubations did not show a significant change in either thio T fluorescence or monomer concentration, indicating that few if any fibrils were formed. At a higher concentration (300 μM), the plus2 variant formed amyloid fibrils, but only after prolonged incubation (data not shown). The mildly agitating conditions of the rotating drum that were chosen for these experiments accelerated fibrillization in every case, but did not change the relative rates of the variants (this has been a general observation in our laboratory in studies of many α-synuclein variants). To confirm this general observation, unagitated incubations of all three variants (70 μM at 37 °C) were followed; the del2 incubations developed thio T reactivity after 15−20 days, while no thio T signal was observed from WT or plus2 incubations after 25 days (Supporting Information).

Changes in the far-UV CD spectra of each protein showed the conversion from random coil to β-sheet structure and paralleled the changes in thio T fluorescence. The del2 variant showed the earliest change of the three, at 18 h (Figure 3C). At 31 h (not shown), the CD spectrum of del2 showed a broad minimum centered at 218 nm, characteristic of a predominantly β-sheet protein, which was increased at 74 h (Figure 3D). WT showed a slight shift to β-sheet structure after 74 h, while plus2 was not significantly changed. At the 74 h time point, the fraction of β-sheet structure for each protein was estimated: 18% in WT, 100% in del2, and 8% in plus2.

Time-dependent changes in aggregate morphology were observed by electron microscopy (Figure 4). Initially, no protofibrillar or fibrillar material was observed in any incubation (not shown). After 18 h, fibrils were visible in the del2 sample, and protofibrils were visible in all samples. At 31 h, protofibrils had disappeared from the del2 sample, and extensive fibrillar structure was observed (del2 protofibrils appeared to have been consumed by 31 h). In contrast, WT and plus2 protofibrils appeared nearly unchanged from 18 to 31 h. After 80 h, clumps of electron-dense material but no elongated fibrils were present in the plus2 sample, but fibrillar structures were observed in the WT sample. The del2 incubation contained numerous fibrils at 80 h.

DISCUSSION

We sought to understand how the N-terminal repeat sequence in α-synuclein affects its structural propensity since its "conformational plasticity" is likely to be important to both its normal and pathogenic functions. Like WT, the monomeric plus2 and del2 variants were unstructured (natively unfolded) in solution. Compared to WT, plus2 disfavors and del2 favors β-sheet structure. Thus, the

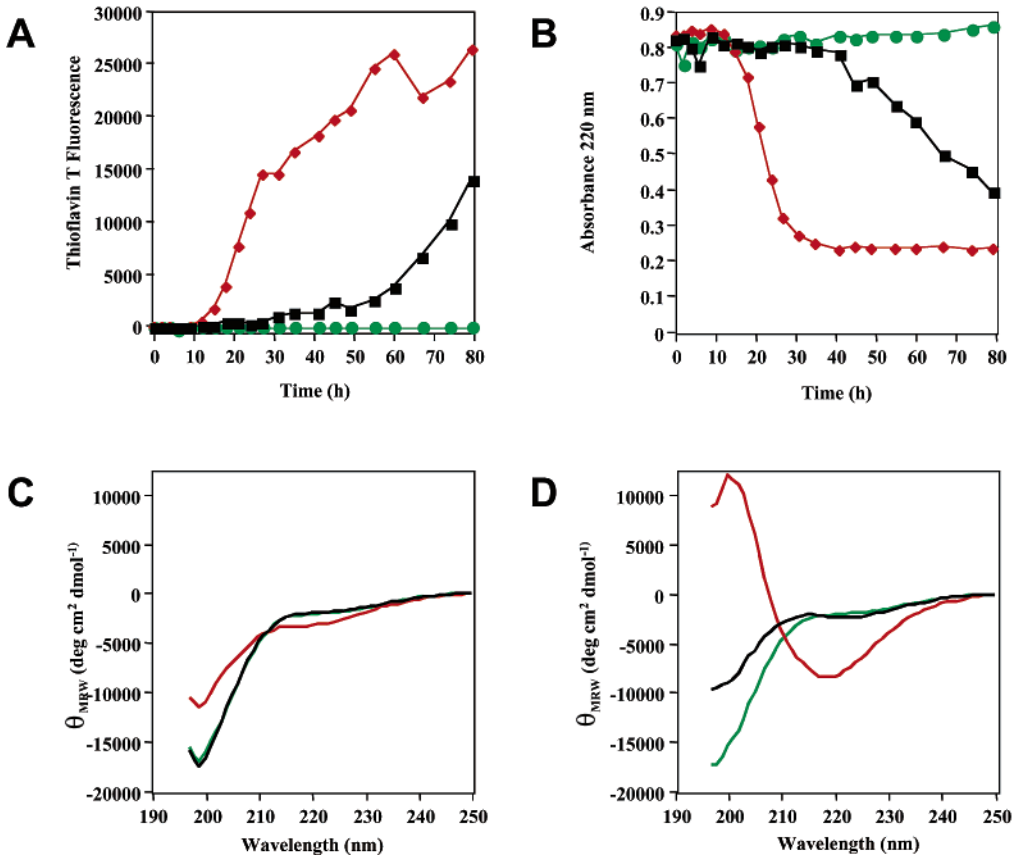

FIGURE 3: Characterization of protein incubations undergoing fibrillization. (A) Thioflavin T fluorescence of aliquots (black for WT, red for del2, and green for plus2) from 80 μM incubations rotating at 37 °C from 0 to 80 h to measure the extent of fibril formation. (B) Peak area of UV absorbance at 220 nm of the monomer peak eluted from a Shodex column. Values for plus2 and del2 were corrected for differences in the extinction coefficient at 220 nm from WT. CD measurements of fibrillization mixtures taken at 18 (C) and 74 h (D). Increases in β-sheet structure content are observed, especially in the del2 sample.

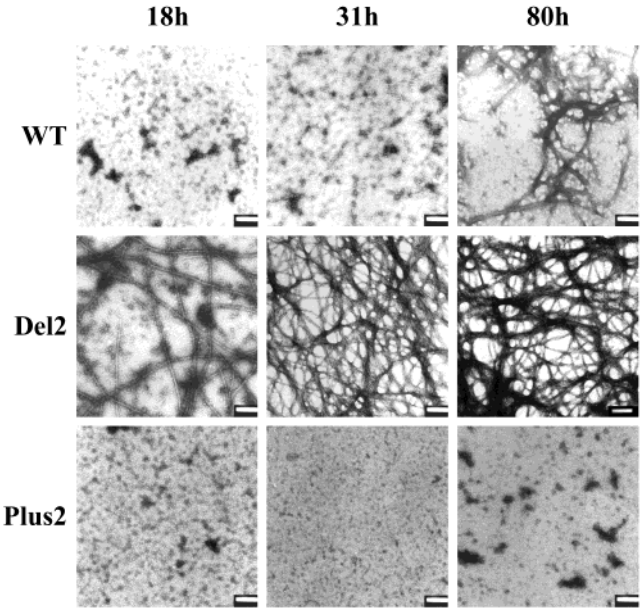

FIGURE 4: Electron microscopy analysis of incubations of WT, del2, and plus2. WT, del2, and plus2 from 80 μM incubations rotating at 37 °C analyzed by electron microscopy at 18, 31, and 80 h time points. Differences in the rate and amount of protofibril and fibril formation are observed. The white bar is 200 nm in length.

N-terminal repeats, which are important for α-helix formation, disfavor the formation of β-sheet-containing structures, including protofibrils and fibrils.

Both FPD mutations (A30P and A53T) lie within the repeated sequence, suggesting either that they increase the inherent fibrillogenicity of the repeats or that they inhibit the ability of the repeats to form a nonpathogenic structure. One version of the latter possibility, that FPD mutations may affect the tendency of the repeats to assume helical secondary structure, was first suggested by Eliezer et al., based on solution NMR chemical shift data that show that the wild-type protein has a tendency toward α-helical structure in the repeat region, which is abolished by the A30P mutation (*30*, *42*). Thus, the A30P mutation may shift the conformational equilibrium away from α-helix, increasing the effective concentration of β-sheet conformers of α-synuclein, and the rate of formation of β-sheet protofibrils. However, the A53T mutation does not change the residual α-helicity as compared to that of WT, and may act by increasing both the rates of monomer-to-protofibril and protofibril-to-fibril transitions (*19*).

Both N-terminal (reported above) and C-terminal (*43*) deletions of α-synuclein increase its fibrillogenicity. This finding is consistent with the fact that the NAC fragment (residues 60−95) is highly fibrillogenic (*44*, *45*) and that this sequence is part of the protease-resistant core of α-synuclein fibrils (*46*). Although the NAC fragment itself may not exist in vivo (*47*), it is important, in light of these data and the isolation of truncated α-synuclein in transgenic mouse brain (*25*), to consider the possibility that truncation of α-synuclein may be involved in pathogenesis of PD or related synucleinopathies.

Accumulating evidence suggests that a discrete protofibrillar form of α-synuclein, the "amyloid pore", may be responsible for PD neurodegeneration (*48*−*52*). The conversion of protofibrils to fibrils may, therefore, act to "detoxify" α-synuclein by consuming the amyloid pores. Both the plus2 and del2 protofibril fractions have pore-like activity in vitro (*48*, *49*), with plus2 being more potent than WT on a per mole basis (J. C. Kessler and P. T. Lansbury, Jr. , unpublished results). Thus, plus2 may show increased pathogenicity as compared to WT in a transgenic animal model (at equal expression levels) where plus2 forms potent pores that are not easily converted to inert fibrils. This hypothesis will be tested in transgenic animal models of PD (*23*, *24*).

Finally, the compromise "choice" of seven repeats that was made by evolution can be rationalized by our "bungee cord" hypothesis (*53*). This choice may reflect the need to avoid overstabilization of the biologically active α-helical conformation, while at the same time decreasing the likelihood of pathogenic protofibril formation.

ACKNOWLEDGMENT

We thank Hilal Lashuel for electron microscopy work and assistance with the fibrillization experiments, Richard Nowak for assistance with fibrillization experiments, Kelly Conway and Mark Shtilerman for assistance with the TMAO experiments, and Margaret Condron for quantitative amino acid analysis.

SUPPORTING INFORMATION AVAILABLE

SDS−PAGE, Western blots, additional CD spectra, and thio T fluorescence measurements from stationary and rotating fibrillization incubations and gel filtration profiles of WT, del2, and plus2. This material is available free of charge via the Internet at http://pubs.acs.org.

REFERENCES

1. Forno, L. S. (1996) *J. Neuropathol. Exp. Neurol. 55*, 259−272.
2. Pollanen, M. S., Dickson, D. W., and Bergeron, C. (1993) *J. Neuropathol. Exp. Neurol. 52*, 183−191.
3. Spillantini, M. G., Schmidt, M. L., Lee, V. M., Trojanowski, J. Q., Jakes, R., and Goedert, M. (1997) *Nature 388*, 839−840.
4. Spillantini, M. G., Crowther, R. A., Jakes, R., Hasegawa, M., and Goedert, M. (1998) *Proc. Natl. Acad. Sci. U.S.A. 95*, 6469−6473.
5. Baba, M., Nakajo, S., Tu, P. H., Tomita, T., Nakaya, K., Lee, V. M., Trojanowski, J. Q., and Iwatsubo, T. (1998) *Am. J. Pathol. 152*, 879−884.
6. Crowther, R. A., Daniel, S. E., and Goedert, M. (2000) *Neurosci. Lett. 292*, 128−130.
7. Maroteaux, L., and Scheller, R. H. (1991) *Brain Res. Mol. Brain Res. 11*, 335−343.
8. Maroteaux, L., Campanelli, J. T., and Scheller, R. H. (1988) *J. Neurosci. 8*, 2804−2815.
9. George, J. M., Jin, H., Woods, W. S., and Clayton, D. F. (1995) *Neuron 15*, 361−372.
10. Jakes, R., Spillantini, M. G., and Goedert, M. (1994) *FEBS Lett. 345*, 27−32.
11. Iwai, A., Masliah, E., Yoshimoto, M., Ge, N., Flanagan, L., de Silva, H. A., Kittel, A., and Saitoh, T. (1995) *Neuron 14*, 467−475.
12. Polymeropoulos, M. H., Lavedan, C., Leroy, E., Ide, S. E., Dehejia, A., Dutra, A., Pike, B., Root, H., Rubenstein, J., Boyer, R., Stenroos, E. S., Chandrasekharappa, S., Athanassiadou, A., Papapetropoulos, T., Johnson, W. G., Lazzarini, A. M., Duvoisin, R. C., Di Iorio, G., Golbe, L. I., and Nussbaum, R. L. (1997) *Science 276*, 2045−2047.
13. Kruger, R., Kuhn, W., Muller, T., Woitalla, D., Graeber, M., Kosel, S., Przuntek, H., Epplen, J. T., Schols, L., and Riess, O. (1998) *Nat. Genet. 18*, 106−108.
14. Kruger, R., Kuhn, W., Leenders, K. L., Sprengelmeyer, R., Muller, T., Woitalla, D., Portman, A. T., Maguire, R. P., Veenma, L., Schroder, U., Schols, L., Epplen, J. T., Riess, O., and Przuntek, H. (2001) *Neurology 56*, 1355−1362.
15. Golbe, L. I., Di Iorio, G., Sanges, G., Lazzarini, A. M., La Sala, S., Bonavita, V., and Duvoisin, R. C. (1996) *Ann. Neurol. 40*, 767−775.
16. Papapetropoulos, S., Paschalis, C., Athanassiadou, A., Papadimitriou, A., Ellul, J., Polymeropoulos, M. H., and Papapetropoulos, T. (2001) *J. Neurol., Neurosurg. Psychiatry 70*, 662−665.
17. Conway, K. A., Harper, J. D., and Lansbury, P. T. (1998) *Nat. Med. 4*, 1318−1320.
18. Conway, K. A., Harper, J. D., and Lansbury, P. T., Jr. (2000) *Biochemistry 39*, 2552−2563.
19. Conway, K. A., Lee, S. J., Rochet, J. C., Ding, T. T., Williamson, R. E., and Lansbury, P. T., Jr. (2000) *Proc. Natl. Acad. Sci. U.S.A. 97*, 571−576.
20. Narhi, L., Wood, S. J., Steavenson, S., Jiang, Y., Wu, G. M., Anafi, D., Kaufman, S. A., Martin, F., Sitney, K., Denis, P., Louis, J. C., Wypych, J., Biere, A. L., and Citron, M. (1999) *J. Biol. Chem. 274*, 9843−9846.
21. Giasson, B. I., Uryu, K., Trojanowski, J. Q., and Lee, V. M. (1999) *J. Biol. Chem. 274*, 7619−7622.
22. Wood, S. J., Wypych, J., Steavenson, S., Louis, J. C., Citron, M., and Biere, A. L. (1999) *J. Biol. Chem. 274*, 19509−19512.
23. Masliah, E., Rockenstein, E., Veinbergs, I., Mallory, M., Hashimoto, M., Takeda, A., Sagara, Y., Sisk, A., and Mucke, L. (2000) *Science 287*, 1265−1269.
24. Feany, M. B., and Bender, W. W. (2000) *Nature 404*, 394−398.
25. Lee, M. K., Stirling, W., Xu, Y., Xu, X., Qui, D., Mandir, A. S., Dawson, T. M., Copeland, N. G., Jenkins, N. A., and Price, D. L. (2002) *Proc. Natl. Acad. Sci. U.S.A. 99*, 8968−8973.
26. Abeliovich, A., Schmitz, Y., Farinas, I., Choi-Lundberg, D., Ho, W. H., Castillo, P. E., Shinsky, N., Verdugo, J. M., Armanini, M., Ryan, A., Hynes, M., Phillips, H., Sulzer, D., and Rosenthal, A. (2000) *Neuron 25*, 239−252.
27. Weinreb, P. H., Zhen, W., Poon, A. W., Conway, K. A., and Lansbury, P. T., Jr. (1996) *Biochemistry 35*, 13709−13715.
28. Davidson, W. S., Jonas, A., Clayton, D. F., and George, J. M. (1998) *J. Biol. Chem. 273*, 9443−9449.
29. Perrin, R. J., Woods, W. S., Clayton, D. F., and George, J. M. (2000) *J. Biol. Chem. 275*, 34393−34398.
30. Eliezer, D., Kutluay, E., Bussell, R., Jr., and Browne, G. (2001) *J. Mol. Biol. 307*, 1061−1073.
31. Li, S. H., and Li, X. J. (1998) *Hum. Mol. Genet. 7*, 777−782.
32. Scherzinger, E., Lurz, R., Turmaine, M., Mangiarini, L., Hollenbach, B., Hasenbank, R., Bates, G. P., Davies, S. W., Lehrach, H., and Wanker, E. E. (1997) *Cell 90*, 549−558.
33. Hutton, M. (2001) *Neurology 56*, S21−S25.
34. Himmler, A., Drechsel, D., Kirschner, M. W., and Martin, D. W., Jr. (1989) *Mol. Cell. Biol. 9*, 1381−1388.
35. Owen, F., Poulter, M., Collinge, J., Leach, M., Lofthouse, R., Crow, T. J., and Harding, A. E. (1992) *Brain Res. Mol. Brain Res. 13*, 155−157.
36. Poulter, M., Baker, H. F., Frith, C. D., Leach, M., Lofthouse, R., Ridley, R. M., Shah, T., Owen, F., Collinge, J., Brown, J., et al. (1992) *Brain 115* (Part 3), 675−685.
37. Chiesa, R., Piccardo, P., Ghetti, B., and Harris, D. A. (1998) *Neuron 21*, 1339−1351.
38. Greenfield, N., and Fasman, G. D. (1969) *Biochemistry 8*, 4108−4116.
39. Gill, S. C., and von Hippel, P. H. (1989) *Anal. Biochem. 182*, 319−326.
40. Baskakov, I., and Bolen, D. W. (1998) *J. Biol. Chem. 273*, 4831−4834.
41. Wang, A., and Bolen, D. W. (1997) *Biochemistry 36*, 9101−9208.
42. Bussell, R., Jr., and Eliezer, D. (2001) *J. Biol. Chem. 276*, 45996−46003.
43. Crowther, R. A., Jakes, R., Spillantini, M. G., and Goedert, M. (1998) *FEBS Lett. 436*, 309−312.
44. Ueda, K., Fukushima, H., Masliah, E., Xia, Y., Iwai, A., Yoshimoto, M., Otero, D. A., Kondo, J., Ihara, Y., and Saitoh, T. (1993) *Proc. Natl. Acad. Sci. U.S.A. 90*, 11282−11286.

45. Han, H., Weinreb, P. H., and Lansbury, P. T., Jr. (1995) *Chem. Biol. 2*, 163−169.
46. Miake, H., Mizusawa, H., Iwatsubo, T., and Hasegawa, M. (2002) *J. Biol. Chem. 277*, 19213−19219.
47. Culvenor, J. G., McLean, C. A., Cutt, S., Campbell, B. C., Maher, F., Jakala, P., Hartmann, T., Beyreuther, K., Masters, C. L., and Li, Q. X. (1999) *Am. J. Pathol. 155*, 1173−1181.
48. Volles, M. J., Lee, S. J., Rochet, J. C., Shtilerman, M. D., Ding, T. T., Kessler, J. C., and Lansbury, P. T., Jr. (2001) *Biochemistry 40*, 7812−7819.
49. Volles, M. J., and Lansbury, P. T., Jr. (2002) *Biochemistry 41*, 4595−4602.
50. Lashuel, H., Petre, B., Wall, J., Simon, M., Nowak, R., Walz, T., and Lansbury, P. (2002) *J. Mol. Biol. 322*, 1089.
51. Lashuel, H. A., Hartley, D., Petre, B. M., Walz, T., and Lansbury, P. T., Jr. (2002) *Nature 418*, 291.
52. Ding, T. T., Lee, S. J., Rochet, J. C., and Lansbury, P. T., Jr. (2002) *Biochemistry 41*, 10209−10217.
53. Lansbury, P. T., Jr. (1999) *Curr. Biol. 9*, R845−R847.

BI020429Y